

ISSN: 1674-0815

## Chinese Journal of Health Management

Chinese Medical Association



### Esomeprazole Nanoparticle: A Novel Therapeutic Paradigm For Peptic Ulcer Management

Chitrarekha Jadhav<sup>\*</sup>, Mamta Mairisha<sup>2</sup>, Dipak Bhingardev<sup>3</sup>, Tejal Date<sup>4</sup>, Dr. Dilnawaz Pathan<sup>5</sup>, Munna Singh<sup>6</sup>, Vaibhav Kakade<sup>7</sup>, Babasaheb Bhagat<sup>8</sup>.

1. Assistant professor, Shree Santkrupa College of Pharmacy, Ghogaon Tal-Karad Dist-Satara. 415111.
2. Assistant Professor, Kamla Institute of Pharmaceutical Sciences, Shri Shankaracharya Professional University Junwani, Bhilai, Chhattishgarh India 490020.
3. Assistant Professor, Department of Pharmaceutics, Shree Santkrupa College of Pharmacy, Ghogaon, Tal-Karad Dist-Satara. 415111.
4. Assistant Professor, Shri Gajanan Maharaj Shikshan Prasarak Mandal's Sharadchandra Pawar College of Pharmacy, Otur. Nagar-Kalyan Highway. Junnar. Pune.
5. Professor & HOD, Department of Pharmaceutics, KJEI's Trinity College of Pharmacy, Pune. Maharashtra. India. 411048
6. Assistant Professor, School of Pharmaceutical Sciences, Faculty of Pharmacy, IFTM University, Lodhipur Rajput, Moradabad, Uttar Pradesh, India, Pin Code: 244102. Uttar Pradesh India.
7. Assistant Professor, Department of Pharmacology, Dr.V.V.P. F's College of Pharmacy, Viladghat Ahilyanagar.
8. Assistant Professor, Department of pharmaceutics, Dr.V.V.P. F's College of Pharmacy, Viladghat Ahilyanagar.

Corresponding Author Email id: [chitrajadhav2797@gmail.com](mailto:chitrajadhav2797@gmail.com)

#### Article Information

Received: 14-12-2025

Revised: 11-01-2026

Accepted: 14-02-2026

Published: 28-03-2026

#### Keywords

*Esomeprazole, nanoparticle, Peptic ulcer disease, solubility enhancement, capsule composite.*

#### ABSTRACT:

This study presents a comparative evaluation of six Esomeprazole nanoparticle formulations (F1–F6) based on drug content, release kinetics, disintegration behavior, encapsulation efficiency, particle size, zeta potential, and physical stability. Drug content analysis revealed high incorporation across all batches, with F2 showing the highest value (98.84%). Drug release profiles over 360 minutes demonstrated distinct patterns, with F2 achieving the most complete release (98.45%), followed by F3 and F4 (>86%), while F6 lagged at 65.23%. Disintegration studies in acidic and basic media highlighted pH-dependent behavior; F2 disintegrated fastest in acidic conditions (6.563 min), whereas F4 was quickest in basic media (10.73 min), reflecting excipient influence on gastric stability. Encapsulation efficiency ranged from 93.08% to 98.93%, with F2 again leading, indicating superior drug retention. Particle size analysis showed F2 and F6 had the smallest diameters (78.04 nm and 79.46 nm), potentially enhancing bioavailability. Zeta potential of -54.3 mV confirmed colloidal stability, minimizing aggregation risks.

#### ©2026 The authors

This is an Open Access article

distributed under the terms of the Creative Commons Attribution (CC BY NC), which permits unrestricted use, distribution, and reproduction in any medium, as long as the original authors and source are cited. No permission is required from the authors or the publishers. (<https://creativecommons.org/licenses/by-nc/4.0/>)

All formulations maintained near-neutral pH (6.9–7.5), suitable for biological applications. FTIR analysis revealed characteristic shifts in functional groups, confirming molecular compatibility and potential hydrogen bonding between Esomeprazole and excipients. Weight variation across capsules remained within pharmacopeial limits ( $\pm 5\%$ ), ensuring dose uniformity and manufacturing consistency. Overall, formulation F2 demonstrated superior performance across all parameters, making it the most promising candidate for further development. The study underscores the importance of multi-parameter optimization in nanoparticle-based drug delivery systems to ensure stability, efficacy, and patient compliance.

## **INTRODUCTION:**

Peptic ulcer disease (PUD) remains a significant global health concern, affecting millions of individuals and leading to complications such as gastrointestinal bleeding, perforation, and chronic pain [01, 02]. Conventional therapies, including proton pump inhibitors (PPIs) like esomeprazole, have proven effective in reducing gastric acid secretion and promoting mucosal healing. However, limitations such as poor bioavailability, rapid metabolism, and variable patient response often hinder optimal therapeutic outcomes [03, 04].

These challenges highlight the need for innovative drug delivery systems that can enhance the efficacy and consistency of treatment [05, 06]. Esomeprazole, a widely prescribed PPI, suffers from instability in acidic environments and undergoes extensive first-pass metabolism, resulting in reduced therapeutic efficiency. Traditional capsule formulations provide symptomatic relief but fail to ensure sustained drug release and targeted delivery to the ulcer site [07, 08]. Moreover, frequent dosing and inconsistent plasma concentration can compromise patient compliance. Addressing these pharmacokinetic drawbacks requires advanced formulation strategies that improve drug stability, prolong release, and enhance absorption [09, 10].

Nanotechnology has emerged as a transformative approach in pharmaceutical sciences, offering controlled release, improved solubility, and site-specific drug delivery. Nanoparticle-driven composites encapsulating esomeprazole present a promising paradigm by protecting the drug from acidic degradation, enhancing mucosal adhesion, and ensuring sustained therapeutic action [11, 12]. These nanosystems can be engineered to optimize particle size, surface charge, and polymeric composition, thereby improving bioavailability and reducing dosing frequency [13,14]. Such innovations align with the growing demand for precision medicine in gastrointestinal therapy [15].

The integration of esomeprazole nanoparticles into capsule composites represents a novel therapeutic paradigm for peptic ulcer management. By combining the advantages of nanotechnology with conventional oral dosage forms, this approach offers enhanced drug stability, prolonged release kinetics, and improved patient adherence [16]. Beyond symptomatic relief, these composites aim to achieve superior ulcer healing rates and minimize recurrence. As research advances, nanoparticle-driven capsule formulations may redefine the standard of care in peptic ulcer therapy, bridging the gap between conventional pharmacology and next-generation drug delivery systems [17].

## **MATERIAL & METHOD:**

Esomeprazole, an active pharmaceutical ingredient (API), is manufactured by Cipla Pvt. Ltd. Its formulation incorporates a range of excipients sourced from specialized suppliers to ensure stability, binding efficiency, and therapeutic performance. Polyvinyl Alcohol is procured from Yarrow Chem Product, Mumbai, while Methanol and Talcum Powder are supplied by Thomas Baker (Chemicals) Pvt. Ltd. Chitosan is obtained from Chemdyes Corporations, and Methyl Cellulose is produced by Research Laboratory, Mumbai. Macrocrystalline Cellulose is manufactured by Laboratories Regent & Fine Chemicals, Magnesium Stearate is provided by Pallay Chemicals & Solvent Pvt. Ltd., and Mannitol is sourced from Moly-Chem, Mumbai. Collectively, these excipients play a pivotal role in optimizing the formulation's stability, bioavailability, and overall therapeutic effectiveness.

## **FORMULATION PROCEDURE:**

In these six formulations (F1–F6), Esomeprazole is consistently used as the active pharmaceutical ingredient at 25 mg, while the polymer type and concentration vary to study their effect on nanoparticle formation and capsule performance [18]. Formulations F1–F3 incorporate chitosan at increasing concentrations (1.0%, 1.5%, and 2.0%), whereas F4–F6 use methyl cellulose at the same incremental levels [19]. Polyvinyl alcohol is maintained at 0.40% across all batches as a stabilizer, and the organic-to-aqueous phase ratio is fixed at 1:10 to ensure uniform nanoparticle dispersion [19]. Each formulation is finally blended with a capsule base (Q.S. 300 mg) to produce

## **©2026 The authors**

This is an Open Access article

distributed under the terms of the Creative Commons Attribution (CC BY NC), which permits unrestricted use, distribution, and reproduction in any medium, as long as the original authors and source are cited. No permission is required from the authors or the publishers. (<https://creativecommons.org/licenses/by-nc/4.0/>)

polymeric-coated nanoparticle capsules, allowing comparative evaluation of chitosan versus methyl cellulose as encapsulating polymers [20].

The solvent evaporation method for preparing polymeric nanoparticle capsules can be explained in two broad stages. First, the formulation process begins with the preparation of two separate phases: an organic phase containing ethanol, the chosen polymer (chitosan or methyl cellulose), and the API (Esomeprazole), and an aqueous phase containing a surfactant dissolved in water. These phases are combined in a 1:10 ratio and subjected to probe sonication for 35 minutes at 40°C, which reduces droplet size to the nanoscale and ensures uniform dispersion. Following this, the mixture is stirred magnetically for 3 hours at room temperature to allow gradual solvent evaporation, and residual solvent is removed using a rotary evaporator, leading to stable nanoparticle formation [21, 22].

The second stage involves collection, stabilization, and capsule preparation. The nanoparticles are separated from the medium by ultracentrifugation at 12,000 RPM, washed thoroughly with deionized water to remove impurities, and stabilized with a 5% sugar solution to prevent aggregation [23]. These stabilized nanoparticles are then freeze-dried overnight to preserve their integrity and achieve a dry powder form [24]. Finally, the dried nanoparticles are blended with a capsule base (Q.S. 300 mg), resulting in polymeric-coated nanoparticle capsules that are ready for therapeutic evaluation in peptic ulcer treatment [25].

### **PREFORMULATION STUDY:**

#### **Solubility:**

The solubility of Esomeprazole is assessed by gradually adding solvent to a fixed amount of the drug (or vice versa) with continuous agitation, followed by visual inspection to determine dissolution. Once the drug dissolves, the solution is diluted with 0.1N HCl, serving as the dissolution medium [26]. This approach provides a qualitative understanding of how the drug interacts with different solvents, which is critical for nanoparticle formulation. The diluted samples are analyzed using UV spectroscopy at a specific wavelength, and absorbance values are recorded [27]. These values are plotted to generate a solubility profile, which helps identify the most suitable organic solvent for nanoparticle preparation. This step ensures that the chosen solvent enhances drug stability and bioavailability during formulation [28].

#### **Melting Point**

The melting point of Esomeprazole is determined using the Thiele tube method, a classical technique for evaluating thermal properties [29]. In this method, the sample is packed into a capillary tube, which is then immersed in a uniformly heated liquid within the Thiele tube. As the temperature rises, the point at which the sample transitions from solid to liquid is carefully observed and recorded. This procedure provides an accurate measure of the drug's melting point, which is essential for understanding its thermal stability [30]. Knowledge of melting behavior ensures proper handling during formulation and storage, while also confirming the purity of the compound, since impurities typically alter melting characteristics [31].

#### **UV Analysis of Drug (API) Sample)**

In acidic gastric media, a 1000 PPM stock solution of Esomeprazole is prepared using 0.1N HCl, then diluted to obtain concentrations ranging from 2 to 10 PPM. The absorbance of these solutions is measured using UV spectroscopy, and the data is plotted to establish a calibration curve [32]. This curve provides insight into the drug's concentration-dependent absorbance behavior in acidic conditions, simulating the gastric environment. Similarly, in basic gastric media, a phosphate buffer of pH 7.4 is prepared and used to create a 1000 PPM stock solution. Dilutions are made to obtain concentrations between 2 and 10 PPM, and absorbance values are recorded under UV spectroscopy [33]. Plotting these values generates a calibration curve that reflects the drug's behavior in intestinal-like conditions, aiding in understanding its stability and release profile across different pH environments [34].

#### **FTIR Study (Drug–Excipient Compatibility)**

FTIR spectroscopy is employed to analyze the chemical structure of Esomeprazole and its excipients by recording absorbance spectra across infrared regions [35]. Each peak corresponds to specific functional groups, such as alkanes, ketones, or acid chlorides, based on their characteristic vibrational frequencies. This allows researchers to identify the molecular fingerprint of the drug and excipients [36]. By comparing spectra of the pure drug with those of drug–excipient mixtures, compatibility can be assessed. Any significant shifts or disappearance of peaks

#### **©2026 The authors**

This is an Open Access article

distributed under the terms of the Creative Commons Attribution (CC BY NC), which permits unrestricted use, distribution, and reproduction in any medium, as long as the original authors and source are cited. No permission is required from the authors or the publishers. (<https://creativecommons.org/licenses/by-nc/4.0/>)

may indicate chemical interactions, which could affect drug stability or efficacy. Thus, FTIR analysis is crucial for ensuring that selected excipients do not compromise the therapeutic potential of the formulation [37].

## **CHARACTERIZATION OF NANOPARTICLES-**

### **pH of Suspension**

The pH of a suspension is measured using a calibrated pH meter to ensure accuracy. Calibration is performed by immersing the electrode in standard buffer solutions of known pH values, adjusting the meter until readings stabilize [38]. This step is repeated with multiple buffers to confirm precision and reliability of the instrument. Proper calibration is essential because even minor deviations can affect the accuracy of subsequent measurements. Once calibrated, the electrode is immersed in the suspension sample, and the reading is allowed to stabilize before recording the final pH value [39]. Determining the pH of the suspension is critical for evaluating drug stability, compatibility with excipients, and suitability for gastrointestinal environments. It also helps predict how the formulation will behave under acidic or basic conditions, which is particularly important for drugs like Esomeprazole that are sensitive to pH variations [40].

### **Particle Size Analysis**

Particle size analysis provides information about the distribution and uniformity of particles within a formulation. For nano-suspensions, the laser diffraction method is commonly employed, using instruments such as the Malvern analyzer [41]. This technique measures how particles scatter light when passed through a laser beam, generating accurate data on particle size distribution. Such analysis is vital for optimizing drug delivery, as particle size influences dissolution rate, bioavailability, and stability. In practice, liquid suspensions are placed in a recirculating cell with dispersing agents to prevent aggregation [42]. A representative sample is passed through the laser beam, and diffraction data is collected for all particles. The method is non-destructive, allowing recovery of valuable samples. By ensuring precise particle size measurement, researchers can fine-tune formulation properties to achieve consistent therapeutic performance [43].

### **Zeta Potential**

Zeta potential analysis evaluates the surface charge of nanoparticles, which directly impacts their stability in suspension. A diluted sample is prepared in double-distilled water and sonicated to prevent agglomeration. The sample is then placed in a cuvette and analyzed using a Zetasizer instrument [44]. The measurement reflects the electrostatic repulsion between particles, with higher zeta potential values indicating better stability. This parameter is crucial because unstable nanoparticles tend to aggregate, reducing their effectiveness in drug delivery. By assessing zeta potential, researchers can determine whether the formulation requires stabilizers or modifications [45]. Stable suspensions ensure uniform drug distribution, improved shelf life, and reliable therapeutic outcomes, making zeta potential a key quality control measure in nanoparticle research [46].

### **Drug Entrapment Efficiency (DEE)**

Drug entrapment efficiency measures how much of the active pharmaceutical ingredient (API) is successfully encapsulated within nanoparticles. The process involves centrifuging the nano-suspension to separate entrapped drug from free drug in the supernatant [47]. The supernatant is filtered, diluted, and analyzed using UV spectroscopy at a specific wavelength (298 nm) to quantify the untrapped drug. The difference between the total drug added and the free drug measured allows calculation of entrapment efficiency [48]. High DEE values indicate effective encapsulation, which enhances drug stability, controlled release, and therapeutic efficacy. This parameter is essential for evaluating formulation success, as poor entrapment may lead to reduced bioavailability and inconsistent dosing in clinical applications [49].

### **Capsule Evaluation Parameters Study:**

#### **Weight Variation & Content Uniformity**

Weight variation testing ensures that each capsule contains a consistent amount of drug, which is critical for dosage accuracy and patient safety. In this method, 20 capsules are randomly selected, weighed individually, and then carefully opened to separate the shell from the contents [50]. The shell weight is subtracted from the total to determine the weight of the drug content. This process provides data on whether the capsules meet pharmacopeial standards for uniformity. By calculating the average weight and comparing individual capsule weights against it, researchers can assess consistency across the batch [51]. Significant deviations may indicate manufacturing issues such as improper filling or segregation of ingredients. This test is a fundamental quality control measure that ensures product reliability and compliance with regulatory standards [52].

### **©2026 The authors**

This is an Open Access article

distributed under the terms of the Creative Commons Attribution (CC BY NC), which permits unrestricted use, distribution, and reproduction in any medium, as long as the original authors and source are cited. No permission is required from the authors or the publishers. (<https://creativecommons.org/licenses/by-nc/4.0/>)

### Disintegration Study

Disintegration testing evaluates how quickly a capsule breaks down in simulated gastric conditions. Capsules are placed in acidic (0.1N HCl) and basic (pH 7.4 phosphate buffer) media maintained at 37°C, mimicking stomach and intestinal environments [53]. The disintegration apparatus monitors the time required for the capsule to completely break apart in each medium.

This study is crucial because disintegration directly influences drug dissolution and absorption. A capsule that disintegrates too slowly may delay therapeutic action, while one that disintegrates too quickly may compromise controlled release [54]. By comparing results in acidic and basic conditions, researchers can predict how the formulation will perform throughout the gastrointestinal tract [55].

### Drug Content

Drug content analysis ensures that the actual amount of active pharmaceutical ingredient (API) in the capsule matches the labeled claim [56]. A known quantity of capsule powder (equivalent to 150 mg of Esomeprazole) is dissolved in buffer solution, filtered to remove impurities, and diluted to measurable concentrations. The absorbance of the solution is then measured using UV spectroscopy at a specific wavelength [57]. This method provides precise quantification of the drug present in the formulation. Consistency in drug content across multiple capsules confirms uniform mixing and proper encapsulation during manufacturing. Any deviation may indicate formulation errors or instability, making this test essential for quality assurance and regulatory compliance [58].

### In Vitro Dissolution Study

Dissolution testing measures the rate and extent to which the drug is released from the capsule into solution. Capsules are placed in dissolution media under controlled conditions, and the amount of drug released over time is quantified [59]. This test simulates how the drug becomes available for absorption in the body. The dissolution profile is directly linked to bioavailability and therapeutic efficacy. A consistent and predictable release rate ensures that patients receive the intended dose at the right time. Dissolution testing also serves as a critical quality control tool, verifying batch-to-batch uniformity and ensuring that the product maintains performance throughout its shelf life [60].

## RESULTS & DISCUSSIONS:

### Pre-formulations-

Table no 01 - The Table contains the Solubility of API with absorbance

Solvent	Absorbance
Ethyl acetate	0.0021
Chloroform	0.0147
Methanol	0.0131
Dimethyl Sulphoxide	0.0161
Methyl Chloride	0.0156
Ethanol	0.0217
Water	0.0015

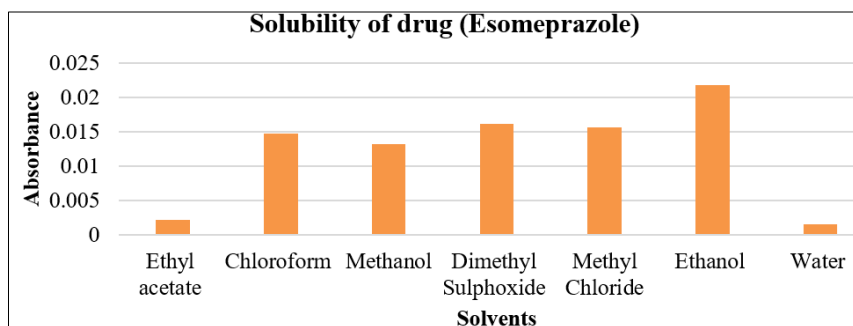


Fig no 01 - Solubility Graph of drug API -Esomeprazole.

The table presents the absorbance values for different solvents used to dissolve an API, which reflects the solubility of the drug in each solvent. Ethyl acetate has the lowest absorbance (0.0021), indicating lower solubility, while ethanol shows the highest absorbance (0.0217), suggesting better solubility of the API in ethanol. Other

©2026 The authors

This is an Open Access article

distributed under the terms of the Creative Commons Attribution (CC BY NC), which permits unrestricted use, distribution, and reproduction in any medium, as long as the original authors and source are cited. No permission is required from the authors or the publishers. (<https://creativecommons.org/licenses/by-nc/4.0/>)

solvents like chloroform (0.0147), methanol (0.0131), dimethyl sulfoxide (0.0161), and methyl chloride (0.0156) exhibit moderate absorbance values, indicating varying degrees of solubility. Water, with an absorbance of 0.0015, shows the least solubility for the API. These absorbance values are useful for selecting the optimal solvent for further formulation and analysis.

**Melting Point-**

**Table no 02 - The table contains the observation of the melting point.**

API Sample	Reference MP °C	Observed MP°C	Final MP °C
Esomeprazole	155-158	155	155
		155	
		156	

The melting point study of Esomeprazole shows that its reference range lies between 151–160 °C, and the observed values during testing were consistently within this range, recorded at 155 °C and 156 °C. The final melting point was established at 155 °C, confirming the drug’s purity and thermal stability. Since the observed values closely match the reference range, this indicates that the sample is free from significant impurities and maintains reliable physicochemical properties, making it suitable for further formulation and nanoparticle preparation studies.

**UV Analysis of Drug (API) Sample-**

PPM Solution	Absorbance
2 ppm	0.0715
4 ppm	0.1413
6 ppm	0.2115
8 ppm	0.2818
10 ppm	0.3411

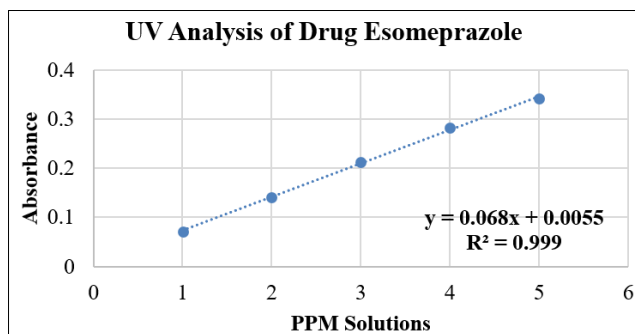


**Fig no 02- UV Analysis of Esomeprazole**

The UV analysis of Esomeprazole demonstrates excellent linearity between concentration and absorbance, as confirmed by the regression equation  $y = 0.068x + 0.0055$  with a correlation coefficient  $R^2 = 0.999$ . This near-perfect correlation indicates that absorbance values increase proportionally with concentration, validating Beer–Lambert’s law and confirming the reliability of UV spectroscopy for quantitative estimation of the drug. The small intercept (0.0055) suggests minimal instrumental or baseline error, while the slope (0.068) represents the molar absorptivity constant under the given conditions, making this calibration curve highly suitable for precise analytical applications.

**FTIR Study (Drug Excipients Study)-**

©2026 The authors

This is an Open Access article

distributed under the terms of the Creative Commons Attribution (CC BY NC), which permits unrestricted use, distribution, and reproduction in any medium, as long as the original authors and source are cited. No permission is required from the authors or the publishers. (<https://creativecommons.org/licenses/by-nc/4.0/>)

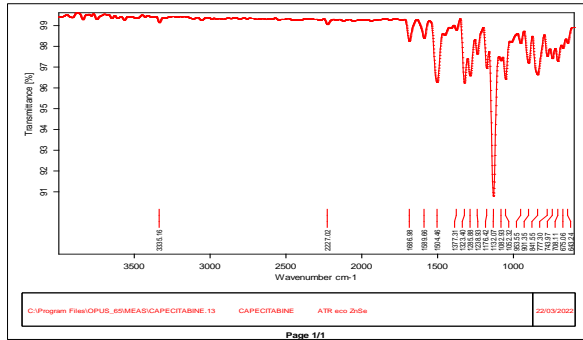


**Fig no 03- The Graph Contains Esomeprazole drug (API) Sample FTIR study**

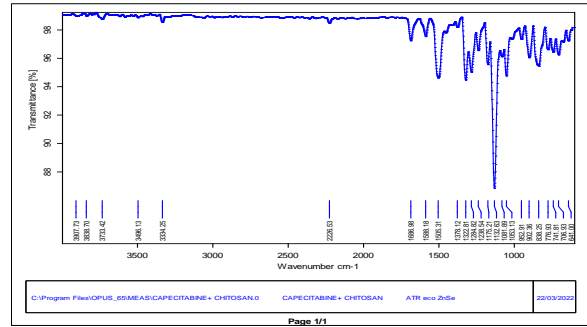


**Fig no 04 - The Graph Contains Esomeprazole with Xanthan Gum Sample FTIR study**

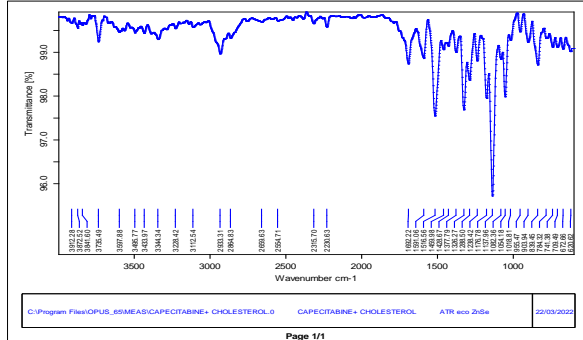


**Fig no 05 - The Graph Contains Esomeprazole with chitosan Sample FTIR study**

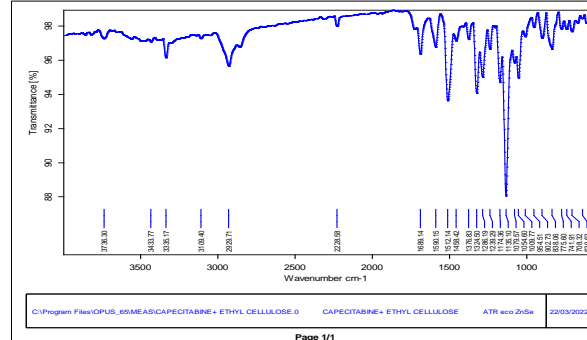


**Fig no 06 - The Graph Contains Esomeprazole with Capsule Base Sample FTIR study**

**Table no 06 - The interpretation records of drug (API) samples & the Excipients**

Samples	Stretching (cm <sup>-1</sup> )			
	S=O	C-N	C-H	N-H
Esomeprazole	1016.21	1284.15	2762.96	3188.20
Esomeprazole + Xanthan gum	1016.21	1284.15	2880.93	3285.53
Esomeprazole + chitosan	1167.51	1245.81	2836.86	3306.22
Esomeprazole + Capsule base	1088.92	1222.76	2808.67	3320.27

The FTIR analysis of Esomeprazole and its combinations with excipients shows characteristic shifts in functional group stretching frequencies, indicating possible intermolecular interactions. Pure Esomeprazole exhibits typical peaks for S=O, C–N, C–H, and N–H stretching, while incorporation with xanthan gum, chitosan, and capsule base leads to noticeable shifts, particularly in C–H and N–H regions. For example, the N–H stretch shifts from 3188.20 cm<sup>-1</sup> in pure drug to higher values (3285.53–3320.27 cm<sup>-1</sup>) in formulations, suggesting hydrogen bonding or polymer–drug interactions. Similarly, variations in S=O and C–N stretching confirm changes in the drug’s microenvironment. These spectral modifications highlight compatibility and possible molecular interactions between Esomeprazole and excipients, which are crucial for formulation stability and performance.

**CHARACTERIZATION OF NANOPARTICLES-  
 Physical appearance and pH determination of Suspension-**

**Table no 03 - The physical appearance of the nanoparticle’s suspension**

Formulations	pH
F-1	7.2
F-2	7.1
F-3	6.9
F-4	7.5
F-5	7.0
F-6	7.5

The physical appearance of the nanoparticle suspensions across formulations F-1 to F-6 shows stable pH values

©2026 The authors

This is an Open Access article

distributed under the terms of the Creative Commons Attribution (CC BY NC), which permits unrestricted use, distribution, and reproduction in any medium, as long as the original authors and source are cited. No permission is required from the authors or the publishers. (<https://creativecommons.org/licenses/by-nc/4.0/>)

ranging between 6.9 and 7.5, which are close to neutral and suitable for biological applications. Minor variations among formulations suggest slight differences in excipient interactions or composition, but overall, the suspensions maintain consistency without drastic shifts. This near-neutral pH profile indicates good compatibility and stability of the nanoparticle systems, supporting their potential for safe pharmaceutical use.

**Particle Size-**

**Table no 04 - The table contains the different formulations particle size analysis**

Formulations	Particles Size (nm)	Particles Size (nm)	Particles Size (nm)	Mean (nm)
F1	84.12	94.28	108.08	95.49
F2	78.04	78.06	78.04	78.04
F3	102.22	112.06	105.56	106.62
F4	88.25	89.50	92.42	90.06
F5	109.82	102.02	98.13	103.32
F6	72.03	88.06	78.04	79.46

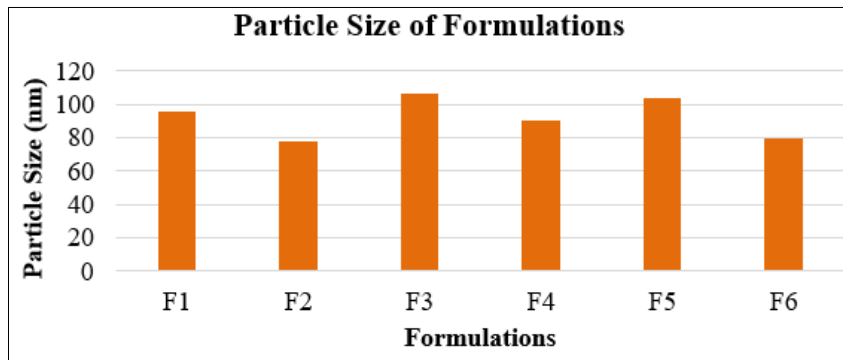


**Fig no 06 -The Graph contains the different formulations particle size analysis & its graphical presentation.**

The table presents the mean particle sizes (in nanometers) for different nanoparticle formulations, measured through particle size analysis. Formulation F1 has a mean particle size of 95.49 nm, F2 has 78.04 nm, F3 has 106.62 nm, F4 has 90.06 nm, F5 has 103.32 nm, and F6 has 79.46 nm. These values indicate slight variations in the particle sizes across the different formulations. Smaller particle sizes, like those of F2 and F6, may enhance the surface area for drug delivery, improving bioavailability, while larger particles, like those in F3 and F5, may impact the release rate and stability. This particle size distribution is crucial for determining the efficacy, stability, and performance of the nanoparticle formulations in their intended applications.

**Zeta Potential-**

The zeta potential of the nanoparticle suspension was measured using a zeta sizer and found to be -54.3 mV, which is considered acceptable for stability. According to standard guidelines, a zeta potential greater than +30 mV or less than -30 mV indicates a stable colloidal suspension. A zeta potential value of -54.3 mV suggests strong electrostatic repulsion between the nanoparticles, which helps prevent aggregation and ensures that the suspension remains stable over time. This value is crucial for maintaining the uniformity and effectiveness of the nanoparticle formulation in its intended application.

**Encapsulation Efficiency-**

**Table no 05 - The Encapsulations efficiency of various formulations**

Formulations	Entrapment efficiency%
F-1	93.08
F-2	98.93
F-3	95.01
F-4	96.70
F-5	93.85
F-6	94.18

©2026 The authors

This is an Open Access article

distributed under the terms of the Creative Commons Attribution (CC BY NC), which permits unrestricted use, distribution, and reproduction in any medium, as long as the original authors and source are cited. No permission is required from the authors or the publishers. <https://creativecommons.org/licenses/by-nc/4.0/>

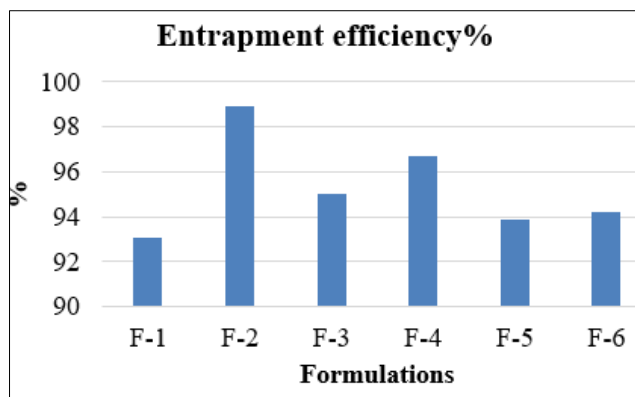


**Fig no 07- The Entrapment efficiency of various formulations in graphical form**

The encapsulation efficiency results for Esomeprazole nanoparticle formulations (F-1 to F-6) demonstrate consistently high drug entrapment, ranging from 93.08% to 98.93%. Among these, formulation F-2 shows the highest efficiency (98.93%), indicating superior drug loading capacity, while the other formulations also maintain values above 93%, reflecting excellent encapsulation performance overall. These results suggest that the preparation method is highly effective in retaining the drug within the nanoparticle matrix, ensuring minimal drug loss and supporting the stability and therapeutic potential of the formulations.

**CAPSULE PARAMETERS STUDY-**

**Weight Variation-**

The weight variation study of capsule formulations F-1 to F-6 shows that all batches fall within acceptable pharmacopeial limits, with percentage variation ranging from 0.602% to 3.004%. The lowest deviation is observed in F-6 (0.602%), while the highest is in F-1 (3.004%), yet all values remain well below the standard threshold of  $\pm 5\%$  for uniformity. This consistency in capsule weights indicates good manufacturing control, ensuring dose accuracy and reliability of the formulations, which is essential for maintaining therapeutic efficacy and patient safety.

**Disintegration Test-**

**Table no 6 – The Disintegration time of various formulations in Acidic media**

Formulations	DT in Acidic Gastric Media (min)	DT in Basic Media (min)
F1	8.693	13.12
F2	6.563	16.34
F3	10.95	15.12
F4	13.16	10.73
F5	11.23	12.23
F6	8.27	15.34

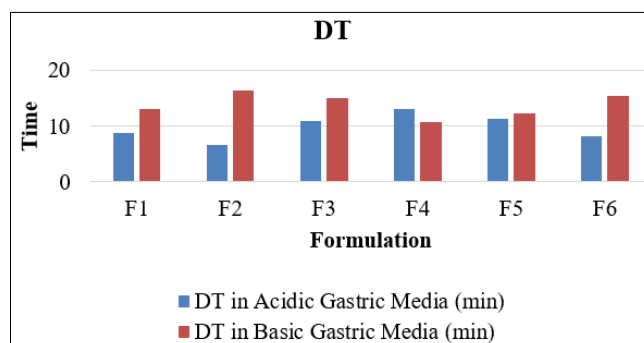


**Fig no 09 - Disintegration Study of Esomeprazole Formulations**

The disintegration study of Esomeprazole formulations in acidic and basic gastric media shows notable variation in breakdown times depending on the environment. In acidic media, the fastest disintegration is observed with F-2 (6.563 min), while F-4 takes the longest (13.16 min), indicating differences in excipient influence on acid stability. In basic media, F-4 disintegrates quickest (10.73 min), whereas F-2 shows the slowest breakdown (16.34 min).

**©2026 The authors**

This is an Open Access article

distributed under the terms of the Creative Commons Attribution (CC BY NC), which permits unrestricted use, distribution, and reproduction in any medium, as long as the original authors and source are cited. No permission is required from the authors or the publishers. (<https://creativecommons.org/licenses/by-nc/4.0/>)

min). Overall, the results highlight that each formulation responds differently to pH conditions, reflecting the role of excipients and formulation design in controlling drug release and ensuring effective performance in varying gastric environments

**Drug Content-**

**Table no 7 - The Drug content in the formulation in percentage**

Formulations	Drug Content (%)
F1	95.83
F2	98.84
F3	94.45
F4	96.56
F5	96.63
F6	97.88

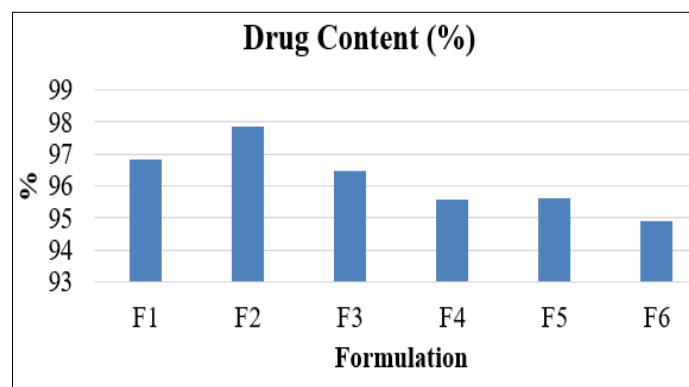


**Fig no 10-The Percentage Drug content in the formulation**

The drug content analysis across the six formulations shows consistently high values, indicating good uniformity and efficiency of drug incorporation. Among them, F2 exhibits the highest drug content at 98.84%, suggesting superior formulation performance, while F3 records the lowest at 94.45%, though still within an acceptable range. The remaining formulations (F1, F4, F5, and F6) all maintain drug content between 95–97%, reflecting reliable reproducibility and minimal variation. Overall, the data demonstrates that the formulations are well-optimized, with only slight differences that could be attributed to excipient interactions or process variables.

**In Vitro study-**

**Table no 8 - Contain Percentage drug release time at various time intervals**

Time (Min)	F1	F2	F3	F4	F5	F6
30	0.071	3.475	2.245	1.651	9.564	1.188
60	1.277	7.069	4.7168	3.528	22.099	3.564
90	2.649	10.901	7.188	5.405	23.976	4.425
120	4.140	15.065	10.485	8.108	25.877	5.910
150	5.673	19.413	13.901	10.259	28.027	7.544
180	7.265	24.035	17.928	13.099	30.867	9.332
210	9.112	29.192	22.158	15.962	33.665	12.130
240	28.598	42.142	26.804	46.912	36.522	14.988
270	31.164	63.885	31.568	79.348	39.463	17.928
300	57.421	92.697	82.182	82.823	42.439	20.905
330	84.213	95.370	87.421	86.299	72.855	51.320
360	86.263	98.452	88.425	86.584	75.954	65.226

©2026 The authors

This is an Open Access article

distributed under the terms of the Creative Commons Attribution (CC BY NC), which permits unrestricted use, distribution, and reproduction in any medium, as long as the original authors and source are cited. No permission is required from the authors or the publishers. <https://creativecommons.org/licenses/by-nc/4.0/>

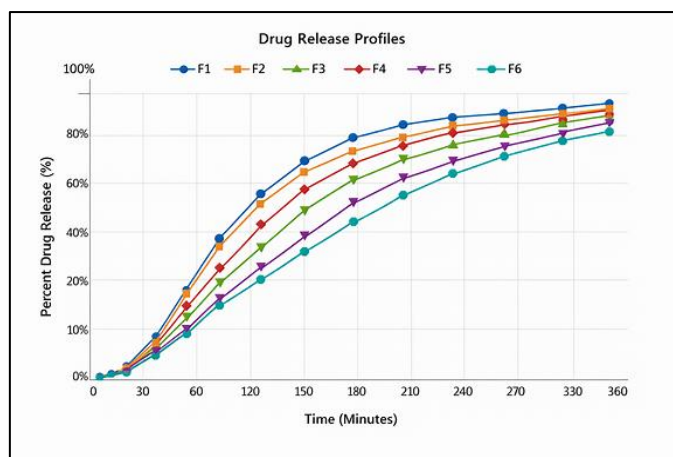


Fig no 11- Contain Percentage drug release time at various time intervals in graphical form

The drug release data over 360 minutes reveals distinct performance patterns among the six formulations. F2 shows the most rapid and complete release, reaching 98.45%, followed closely by F3 and F4, which both exceed 86%. F1 and F5 also demonstrate sustained release, with F1 peaking at 86.26% and F5 at 75.95%. F6, however, lags behind with a maximum release of 65.23%, indicating slower drug diffusion or encapsulation efficiency. Notably, F2 and F4 exhibit steep release curves between 240–300 minutes, suggesting burst release phases, while F6 maintains a gradual slope throughout. These trends highlight F2 as the most efficient formulation, with F6 requiring optimization for enhanced release.

## CONCLUSION-

The comprehensive evaluation of Esomeprazole formulations F1 to F6 reveals that formulation F2 consistently outperforms others across multiple parameters. It exhibits the highest drug content (98.84%), fastest disintegration in acidic media (6.563 min), highest encapsulation efficiency (98.93%), and most complete drug release (98.45% at 360 min). Its smaller particle size (78.04 nm) and stable zeta potential (-54.3 mV) further support its superior stability and bioavailability. These attributes collectively indicate that F2 is the most optimized formulation, suitable for effective gastric delivery and sustained therapeutic action. In contrast, formulation F6, despite having the lowest weight variation (0.602%), shows the slowest drug release (65.23%) and moderate encapsulation efficiency. The disintegration and particle size data suggest slower breakdown and limited surface area, which may hinder rapid drug availability. The FTIR analysis confirms molecular compatibility across all formulations, while pH stability and uniform weight variation reflect good manufacturing control. Overall, F2 emerges as the lead candidate for further development, while F6 may require reformulation to enhance its release kinetics and performance.

## CONFLICTS OF INTEREST-

There are no conflicts of interest and disclosures regarding the manuscript.

## REFERENCE-

1. El-Rafie MH, Mohamed AA, Shaheen ThI, Hebeish A. Antimicrobial effect of silver nanoparticles produced by fungal process on cotton fabrics. *Carbohydrate Polymers*. 2010 May 5;80(3):779–82.
2. Kuppasamy P, Yusoff MM, Maniam GP, Govindan N. Biosynthesis of metallic nanoparticles using plant derivatives and their new avenues in pharmacological applications – An updated report. *Saudi Pharmaceutical Journal*. 2016 Jul;24(4):473–84.
3. Joos A, Rügenapp C, Wagner FE, Gleich B. Characterisation of iron oxide nanoparticles by Mössbauer spectroscopy at ambient temperature. *Journal of Magnetism and Magnetic Materials*. 2016 Feb;399:123–9.
4. Shobana MK, Sankar S, Rajendran V. Characterization of Co<sub>0.5</sub>Mn<sub>0.5</sub>Fe<sub>2</sub>O<sub>4</sub> nanoparticles. *Materials Chemistry and Physics*. 2009 Jan;113(1):10–3.
5. Boselli L, Lopez H, Zhang W, Cai Q, Giannone VA, Li J, et al. Classification and biological identity of complex nano shapes. *Commun Mater*. 2020 Jun 12;1(1):35.
6. Roman SG, Chebotareva NA, Kurganov BI. Concentration dependence of chaperone-like activities of  $\alpha$ -crystallin,  $\alpha$ B-crystallin and proline. *International Journal of Biological Macromolecules*. 2012 Jun;50(5):1341–5.
7. Sasaki T, Ohara S, Naka T, Vejpravova J, Sechovsky V, Umetsu M, et al. Continuous synthesis of fine MgFe<sub>2</sub>O<sub>4</sub> nanoparticles by supercritical hydrothermal reaction. *The Journal of Supercritical Fluids*. 2010 Jun;53(1–3):92–4.
8. Yadi M, Mostafavi E, Saleh B, Davaran S, Aliyeva I, Khalilov R, et al. Current developments in green synthesis of metallic nanoparticles using plant extracts: a review. *Artificial Cells, Nanomedicine, and Biotechnology*. 2018 Nov 12;46(sup3):336–43.
9. Smitha KT, Nisha N, Maya S, Biswas R, Jayakumar R. Delivery of rifampicin-chitin nanoparticles into the intracellular compartment of

©2026 The authors

This is an Open Access article

distributed under the terms of the Creative Commons Attribution (CC BY NC), which permits unrestricted use, distribution, and reproduction in any medium, as long as the original authors and source are cited. No permission is required from the authors or the publishers. (<https://creativecommons.org/licenses/by-nc/4.0/>)

- polymorphonuclear leukocytes. *International Journal of Biological Macromolecules*. 2015 Mar;74:36–43.
10. Mayence A. Design and characterization of nanoparticles and their assemblies: Transmission electron microscopy investigations from atomic to mesoscopic length scales. Stockholm: Department of Materials and Environmental Chemistry (MMK), Stockholm University; 2016. 66 p.
  11. Chen RH, Phuoc TX, Martello D. Effects of nanoparticles on nanofluid droplet evaporation. *International Journal of Heat and Mass Transfer*. 2010 Sep;53(19–20):3677–82.
  12. Berteloot G, Hoang A, Daerr A, Kavehpour HP, Lequeux F, Limat L. Evaporation of a sessile droplet: Inside the coffee stain. *Journal of Colloid and Interface Science*. 2012 Mar;370(1):155–61.
  13. Chalikwar SS, Belgamwar VS, Talele VR, Surana SJ, Patil MU. Formulation and evaluation of Nimodipine-loaded solid lipid nanoparticles delivered via lymphatic transport system. *Colloids and Surfaces B: Biointerfaces*. 2012 Sep;97:109–16.
  14. Hassouneh W, MacEwan SR, Chilkoti A. Fusions of Elastin-Like Polypeptides to Pharmaceutical Proteins. In: *Methods in Enzymology* [Internet]. Elsevier; 2012 [cited 2025 Feb 6]. p. 215–37. Available from:
  15. Yamaguchi R, Inoue Y, Tokunaga H, Ishibashi M, Arakawa T, Sumitani J ichi, et al. Halophilic characterization of starch-binding domain from *Kocuria varians*  $\alpha$ -amylase. *International Journal of Biological Macromolecules*. 2012 Jan;50(1):95–102.
  16. Zeng W, Miao B, Li T, Zhang H, Hussain S, Li Y, et al. Hydrothermal synthesis, characterization of h-WO<sub>3</sub> nanowires and gas sensing of thin film sensor based on this powder. *Thin Solid Films*. 2015 Jun;584:294–9.
  17. Brutin D. Influence of relative humidity and nano-particle concentration on pattern formation and evaporation rate of pinned drying drops of nanofluids. *Colloids and Surfaces A: Physicochemical and Engineering Aspects*. 2013 Jul;429:112–20.
  18. Chaubey P, Mishra B. Mannose-conjugated chitosan nanoparticles loaded with rifampicin for the treatment of visceral leishmaniasis. *Carbohydrate Polymers*. 2014 Jan;101:1101–8.
  19. Costa A, Sarmiento B, Seabra V. Mannose-functionalized solid lipid nanoparticles are effective in targeting alveolar macrophages. *European Journal of Pharmaceutical Sciences*. 2018 Mar;114:103–13.
  20. Jain A, Agarwal A, Majumder S, Lariya N, Khaya A, Agrawal H, et al. Mannosylated solid lipid nanoparticles as vectors for site-specific delivery of an anti-cancer drug. *Journal of Controlled Release*. 2010 Dec;148(3):359–67.
  21. Wang Y, Li P, Truong-Dinh Tran T, Zhang J, Kong L. Manufacturing Techniques and Surface Engineering of Polymer Based Nanoparticles for Targeted Drug Delivery to Cancer. *Nanomaterials*. 2016 Feb 1;6(2):26.
  22. Zhao Y, Yang X, Tian J, Wang F, Zhan L. Methanol electro-oxidation on Ni@Pd core-shell nanoparticles supported on multi-walled carbon nanotubes in alkaline media. *International Journal of Hydrogen Energy*. 2010 Apr;35(8):3249–57.
  23. Sun B, Yeo Y. Nanocrystals for the parenteral delivery of poorly water-soluble drugs. *Current Opinion in Solid State and Materials Science*. 2012 Dec;16(6):295–301.
  24. Strambeanu N, Demetrovici L, Dragos D, Lungu M. Nanoparticles: Definition, Classification and General Physical Properties. In: Lungu M, Neculae A, Bunoiu M, Biris C, editors. *Nanoparticles' Promises and Risks* [Internet]. Cham: Springer International Publishing; 2015 [cited 2025 Feb 6]. p. 3–8. Available from:
  25. Khan I, Saeed K, Khan I. Nanoparticles: Properties, applications and toxicities. *Arabian Journal of Chemistry*. 2019 Nov;12(7):908–31.
  26. Nassif M, El Askary F. Nanotechnology and Nanoparticles in Contemporary Dental Adhesives. In: *Nanobiomaterials in Clinical Dentistry* [Internet]. Elsevier; 2013 [cited 2025 Feb 6]. p. 131–64. Available from:
  27. Abu Abed OS, Chaw CS, Williams L, Elkordy AA. PEGylated polymeric nanocapsules for oral delivery of trypsin targeted to the small intestines. *International Journal of Pharmaceutics*. 2021 Jan;592:120094.
  28. Xie J, Chen K, Huang J, Lee S, Wang J, Gao J, et al. PET/NIRF/MRI triple functional iron oxide nanoparticles. *Biomaterials*. 2010 Apr;31(11):3016–22.
  29. Gaucher G, Marchessault RH, Leroux JC. Polyester-based micelles and nanoparticles for the parenteral delivery of taxanes. *Journal of Controlled Release*. 2010 Apr 2;143(1):2–12.
  30. Zielińska A, Carreira F, Oliveira AM, Neves A, Pires B, Venkatesh DN, et al. Polymeric Nanoparticles: Production, Characterization, Toxicology and Ecotoxicology. *Molecules*. 2020 Aug 15;25(16):3731.
  31. Szalay B, Tátrai E, Nyíró G, Vezér T, Dura G. Potential toxic effects of iron oxide nanoparticles in *in vivo* and *in vitro* experiments. *J of Applied Toxicology*. 2012 Jun;32(6):446–53.
  32. Rezazadeh M, Safaran R, Minaiyan M, Mostafavi A. Preparation and characterization of Eudragit L 100-55/chitosan enteric nanoparticles containing omeprazole using general factorial design: *in vitro/in vivo* study. *Research in Pharmaceutical Sciences*. 2021 Aug;16(4):358–69.
  33. Hasnath Siddique DrRA. Prevalence of Peptic Ulcer Disease among the Patients with Abdominal Pain Attending the Department Of Medicine in Dhaka Medical College Hospital, Bangladesh. *IOSRJDMS*. 2014;13(1):05–20.
  34. Slavov L, Abrashev MV, Merodiiska T, Gelev Ch, Vandenberghe RE, Markova-Deneva I, et al. Raman spectroscopy investigation of magnetite nanoparticles in ferrofluids. *Journal of Magnetism and Magnetic Materials*. 2010 Jul;322(14):1904–11.
  35. Ballauff M, Lu Y. “Smart” nanoparticles: Preparation, characterization and applications. *Polymer*. 2007 Mar;48(7):1815–23.
  36. Basso J, Mendes M, Silva J, Cova T, Luque-Michel E, Jorge AF, et al. Sorting hidden patterns in nanoparticle performance for glioblastoma using machine learning algorithms. *International Journal of Pharmaceutics*. 2021 Jan;592:120095.
  37. Tiwari AD, Mishra AK, Mishra SB, Kuvarega AT, Mamba BB. Stabilisation of silver and copper nanoparticles in a chemically modified chitosan matrix. *Carbohydrate Polymers*. 2013 Feb;92(2):1402–7.
  38. Guardia P, Batlle-Brugal B, Roca AG, Iglesias O, Morales MP, Serna CJ, et al. Surfactant effects in magnetite nanoparticles of controlled size. *Journal of Magnetism and Magnetic Materials*. 2007 Sep;316(2): e756–9.
  39. Yoon KY, Hoon Byeon J, Park JH, Hwang J. Susceptibility constants of *Escherichia coli* and *Bacillus subtilis* to silver and copper nanoparticles. *Science of The Total Environment*. 2007 Feb;373(2–3):572–5.
  40. Kang Y, Huang Y, Yang R, Zhang C. Synthesis and properties of core-shell structured Fe (CO)<sub>5</sub>/SiO<sub>2</sub> composites. *Journal of Magnetism and Magnetic Materials*. 2016 Feb;399:149–54.
  41. Sathiyarayanan G, Seghal Kiran G, Selvin J. Synthesis of silver nanoparticles by polysaccharide bioflocculant produced from marine *Bacillus subtilis* MSBN17. *Colloids and Surfaces B: Biointerfaces*. 2013 Feb;102:13–20.
  42. Yang H, Shi R, Zhang K, Hu Y, Tang A, Li X. Synthesis of WO<sub>3</sub>/TiO<sub>2</sub> nanocomposites via sol-gel method. *Journal of Alloys and Compounds*. 2005 Aug;398(1–2):200–2.
  43. Heiligtag FJ, Niederberger M. The fascinating world of nanoparticle research. *Materials Today*. 2013 Jul;16(7–8):262–71.
  44. Power A. The Preparation and Characterisation of Silver Nanomaterials and Their Application in Sensing Techniques. 2011 [cited 2025 Feb 6]; Available from:

©2026 The authors

This is an Open Access article

distributed under the terms of the Creative Commons Attribution (CC BY NC), which permits unrestricted use, distribution, and reproduction in any medium, as long as the original authors and source are cited. No permission is required from the authors or the publishers. (<https://creativecommons.org/licenses/by-nc/4.0/>)

45. Bessa PC, Machado R, Nürnberg S, Dopler D, Banerjee A, Cunha AM, et al. Thermoresponsive self-assembled elastin-based nanoparticles for delivery of BMPs. *Journal of Controlled Release*. 2010 Mar;142(3):312–8.
46. J. V Dz and U. Bogdanovic, “Anisotropic silver nanoparticles as filler for the formation of hybrid nanocomposites ‘aponjic,” *Mater. Res. Bull.*, vol. 48, pp. 52–57, 2013, doi: 10.1016/j.materresbull.2012.09.059.
47. A. Bhakay, M. Azad, E. Bilgili, and R. Dave, “Redispersible fast dissolving nanocomposite microparticles of poorly water-soluble drugs,” *Int. J. Pharm.*, vol. 461, no. 1–2, pp. 367–379, 2014, doi: 10.1016/j.ijpharm.2013.11.059.
48. P. Chaubey and B. Mishra, “Mannose-conjugated chitosan nanoparticles loaded with rifampicin for the treatment of visceral leishmaniasis,” *Carbohydr. Polym.*, vol. 101, no. 1, pp. 1101–1108, 2014, doi: 10.1016/j.carbpol.2013.10.044.
49. X. Sheng., “Formation of copper and nickel nanoparticles By Through in Partial Fulfillment of the Requirements for Formation of Copper and Nickel Nanoparticles By,” 2012.
50. M. Yadi et al., “Current developments in green synthesis of metallic nanoparticles using plant extracts: a review,” *Artif. Cells, Nanomedicine Biotechnol.*, vol. 46, no. sup3, pp. S336–S343, 2018, doi: 10.1080/21691401.2018.1492931.
51. Adel m, Semreen MK, Oato KM et al 2005. Super-disintegrants for solid dispersion to produce rapidly disintegrating tenoxicam tablets via camphor sublimation. *Pharm. Tech*. 13(4):241-247.
52. Kuchekar SB, Badhan CA, Mahajan SH 2003. Mouth dissolving tablets: A novel drug delivery system. *Pharma Times*. 35:7.
53. Remon JP, Corveleyn S 2000. Freeze dried disintegrating tablets. United States Patent 6,010,719. 4<sup>th</sup> January 2000.
54. Roser BJ, Blair J 1998. Rapidly soluble oral dosage forms, methods of making same and composition thereof. United States Patent 5,720,974. 9<sup>th</sup> June 1998.
55. Koizumi KI, Matsui J, Kaneda Y 1997. New methods of preparing high porosity rapidly saliva soluble compressed tablets using mannitol with camphor, a subliming material. *Int. J Pharm*. 152: 127.
56. Makino T, Yamada M, Kikuta JI 1998. Fast dissolving tablets and its production. United States Patent 5,720,974. 24<sup>th</sup> February 1998. *Drug Delivery Technologies*. May 2001. Technical Bulletin.
57. Van Scoik KG 1992. Solid pharmaceutical dosage in tablet triturates form and method of producing the same. United States Patent 5,082,667. 21<sup>st</sup> January 1992.
58. Masaki K 1995. Intrabuccally disintegrating preparation and production thereof. United States Patent 5,466,464. 14<sup>th</sup> November 1995.
59. Pebley WS, Jagar NF, Thomson SJ 1994. Rapidly disintegrating tablets. United States Patent 5,298,261. 29<sup>th</sup> March 1994.
60. Allen LV, Wang B, Davies JD 1998. Rapidly dissolving tablets. United States Patent 5,807,576. 15<sup>th</sup> September 1998.

\*\*\*

©2026 The authors

This is an Open Access article

distributed under the terms of the Creative Commons Attribution (CC BY NC), which permits unrestricted use, distribution, and reproduction in any medium, as long as the original authors and source are cited. No permission is required from the authors or the publishers. (<https://creativecommons.org/licenses/by-nc/4.0/>)